1521-0103/379/1/53–63$35.00
THE JOURNAL OF PHARMACOLOGY AND EXPERIMENTAL THERAPEUTICS

https://doi.org/10.1124/jpet.121.000790
J Pharmacol Exp Ther 379:53–63, Month 2021

The Journal of PHARMACOLOGY And Experimental Therapeutics

Protein Kinase N Family Negatively Regulates Constitutive Androstane Receptor-Mediated Transcriptional Induction of Cytochrome P450 2b10 in the Livers of Mice[S]

Atsushi Kawase, Hideyuki Mukai,[1] Shunsuke Tateishi, Shintaro Kuroda, Akira Kazaoka, Ryosuke Satoh, Hiroaki Shimada, Reiko Sugiura, and Masahiro Iwaki[1]

[1]Department of Pharmacy, Faculty of Pharmacy, Kindai University, Osaka, Japan (A.Kaw., S.T., S.K., A.Kaz., H.S., M.I.); Biosignal Research Center, Kobe University, Hyogo, Japan (H.M.); Department of Clinical Laboratory, Kitano Hospital, Osaka, Japan (H.M.); Department of Pharmaceutical Sciences, Faculty of Pharmacy, Kindai University, Osaka, Japan (R.Sa., R.Su.); Pharmaceutical Research and Technology Institute, Kindai University, Osaka, Japan (R.Su., M.I.); and Antiaging Center, Kindai University, Osaka, Japan (R.Su., M.I.)

Received June 10, 2021; accepted July 22, 2021

ABSTRACT

In receptor-type transcription factors–mediated cytochrome P450 (P450) induction, few studies have attempted to clarify the roles of protein kinase N (PKN) in the transcriptional regulation of P450s. This study aimed to examine the involvement of PKN in the transcriptional regulation of P450s by receptor-type transcription factors, including the aryl hydrocarbon receptor, constitutive androstane receptor (CAR), and pregnane X receptor. The mRNA and protein levels and metabolic activity of P450s in the livers of wild-type (WT) and double-mutant (D) mice harboring both PKN1 kinase-negative knock-in and PKN3 knockout mutations [*PKN1*$^{T778A/T778A}$; *PKN3*$^{-/-}$] were determined after treatment with activators for receptor-type transcription factors. mRNA and protein levels and metabolic activity of CYP2B10 were significantly higher in D mice treated with the CAR activator phenobarbital (PB) but not with 1,4-bis((3,5-dichloropyridin-2-yl)oxy)benzene compared with WT mice. We examined the CAR-dependent pathway regulated by PKN after PB treatment because the extent of CYP2B10 induction in WT and D mice was notably different in response to treatment with different CAR activators. The mRNA levels of *Cyp2b10* in primary hepatocytes from WT and D mice treated with PB alone or in combination with Src kinase inhibitor 1 (SKI-1) or U0126 (a mitogen-activated protein kinase inhibitor) were evaluated. Treatment of hepatocytes from D mice with the combination of PB with U0126 but not SKI-1 significantly increased the mRNA levels of *Cyp2b10* compared with those from the corresponding WT mice. These findings suggest that PKN may have inhibitory effects on the Src–receptor for activated C kinase 1 (RACK1) pathway in the CAR-mediated induction of *Cyp2b10* in mice livers.

SIGNIFICANCE STATEMENT

This is the first report of involvement of PKN in the transcriptional regulation of P450s. The elucidation of mechanisms responsible for induction of P450s could help optimize the pharmacotherapy and improve drug development. We examined whether the mRNA and protein levels and activities of P450s were altered in double-mutant mice harboring both PKN1 kinase-negative knock-in and PKN3 knockout mutations. PKN1/3 negatively regulates CAR-mediated induction of Cyp2b10 through phosphorylation of a signaling molecule in the Src-RACK1 pathway.

Introduction

Protein kinases regulate various proteins involved in the proliferation, infiltration, and metastasis of cancer cells via phosphorylation (Itoh et al., 1999; Raffetto et al., 2006; Santel et al., 2010; Steelman et al., 2011) and account for approximately 60% of molecular targets for cancer drugs. Protein kinase N (PKN) is a serine/threonine-protein kinase with a catalytic domain that is highly homologous to that of protein kinase C at its C-terminal region, three repeats of an

This work was supported by the MEXT-Supported Program for the Strategic Research Foundation at Private Universities, 2014–2018 [Grant S1411037].
The authors declare no competing interest.
[1]M.I. and H.M. contributed equally to this work.
https://dx.doi.org/10.1124/jpet.121.000790.
[S] This article has supplemental material available at jpet.aspetjournals.org.

ABBREVIATIONS: AhR, aryl hydrocarbon receptor; AMPK, AMP-activated protein kinase; BNF, β-naphthoflavone; BUP, bupropion; CAR, constitutive androstane receptor; CCRP, cytoplasmic CAR retention protein; D, double-mutant; DEX, dexamethasone; DIC, diclofenac; EGF, epidermal growth factor; EGFR, epidermal growth factor receptor; ERK, extracellular signal-regulated kinase; HSP, heat shock protein; K_m, Michaelis constant; LC-MS/MS, liquid chromatography–tandem mass spectrometry; MEK, mitogen-activated protein kinase; P450, cytochrome P450; P-ERK, phosphorylated-ERK; P-RACK, phosphorylated-RACK; PB, phenobarbital; PHE, phenacetin; PKN, protein kinase N; PPAR-α, peroxisome proliferator-activated receptor-α; PXR, pregnane X receptor; RACK1, receptor for activated C kinase 1; RXR, retinoid X receptor; SKI-1, Src kinase inhibitor 1; TCPOBOP, 1, 4-bis (((3, 5-dichloropyridin-2-yl)oxy)) benzene; TES, testosterone; WT, wild type.

antiparallel coiled-coil finger domain, and a C2-like domain at its N-terminal region (Maesaki et al., 1999; Mukai, 2003). In mammals, PKN exists in three subtypes (PKN1/PKNα/PRK1/PAK1, PKN2/PRK2/PAK2/PKNγ, and PKN3/PKNβ). mRNA of PKN1, PKN2, and PKN3 is expressed ubiquitously in the brain, liver, lung, spleen, kidney, heart, intestine, testis, and skeletal muscle (Mukai et al., 2016). Compared with classic protein kinases, such as protein kinase A and protein kinase C, the physiologic roles of PKN have not been clarified; however, our group and others have identified some physiologic roles for this protein kinase (Mukai et al., 2016; Quétier et al., 2016; Danno et al., 2017; Mashud et al., 2017; Uehara et al., 2017). To elucidate the detailed physiologic roles of PKN, newly generated double-mutant (D) mice harboring both PKN1 kinase-negative knock-in and PKN3 knockout mutations [*PKN1*$^{T778A/T778A}$; *PKN3*$^{-/-}$] were used in this study. D mice developed into fertile adults and were morphologically indistinguishable from their wild-type (WT) counterparts. Conversely, PKN2 knockout mice are not viable due to lethality by embryonic day 10.5. The previous report suggested that PKNs were activated by Rho family GTPases, fatty acid, 3-phosphoinositide-dependent kinase 1, and mammalian target of rapamycin or cleavage by caspase 3–like protease (Mukai, 2003). In the association between epidermal growth factor receptor (EGFR) signal and PKN, it has been reported that the internalization of EGFR is regulated by PKN1 (Gampel et al., 1999).

The expression of cytochrome P450 (P450), which is involved in the oxidative metabolism of various endogenous and exogenous compounds, is modulated by genetic variations between individuals and in response to drugs (Sheweita, 2000; McGraw and Waller, 2012). Drug-drug interactions can result in the induction or inhibition of P450 expression. Previous studies have demonstrated that P450s are regulated by kinases on many levels, including transcriptional regulation, protein degradation, and cellular signaling (Ding and Staudinger, 2005; Oesch-Bartlomowicz and Oesch, 2008; Wang et al., 2009; Müller et al., 2017; Che and Dai, 2019; Smutny et al., 2021). Receptor-type transcription factors, such as aryl hydrocarbon receptor (AhR), and nuclear receptor gene superfamily, such as constitutive androstane receptor (CAR, NR1I3) and pregnane X receptor (PXR, NR1I2), predominantly regulate the transcription of P450s. CAR and PXR are classified as nuclear receptors. The functions of receptor-type transcription factors are modulated by phosphorylation. For example, the phosphorylation of AhR is required to activate AhR function after treatment with AhR ligands, such as β-naphthoflavone (BNF) (Long et al., 1998; Schrenk, 1998; Lemaire et al., 2004). Stimulating cells with CAR activators, such as phenobarbital (PB, an indirect activator of CAR) and 1,4-bis((3,5-dichloropyridin-2-yl)oxy)benzene (TCPOBOP, a direct CAR ligand in mice), leads to the translocation of CAR from the cytoplasm to the nucleus after dephosphorylation of the CAR complex (Kawamoto et al., 1999; Tzameli et al., 2000; Yoshinari et al., 2003; Numazawa et al., 2005). The transcriptional regulation of P450s is negatively regulated by PXR phosphorylation (Ding and Staudinger, 2005; Lin et al., 2008; Lichti-Kaiser et al., 2009; Staudinger et al., 2011). Activation of PXR by ligands, such as dexamethasone (DEX), upregulates the transcription of target P450s (Down et al., 2007; Scheer et al., 2010). However, it is unclear whether PKN participates in the transcriptional and post-translational regulation of P450 expression and activity via the activation of receptor-type transcription factors.

This prompted us to clarify the roles of PKN in the transcriptional regulation of P450 expression by AhR, CAR, and PXR. We examined the mRNA and protein levels and metabolic activity of P450s in the livers of D mice treated with BNF, PB, TCPOBOP, and DEX. We chose the P450s involved in the metabolism of xenobiotics, such as drugs, because these P450s are important for elucidating drug-drug interactions.

Materials and Methods

Chemicals and Reagents. BNF, phenacetin (PHE), acetaminophen, corn oil, and Sepasol-RNA I Super G were purchased from Nacalai Tesque (Kyoto, Japan). PB, DEX, diclofenac (DIC), protease inhibitor cocktail, and Williams' Medium E were obtained from Sigma-Aldrich (St. Louis, MO). Fast SYBR Green Master Mix, BCA protein assay kit, and GlutaMAX supplement I were obtained from Life Technologies (Carlsbad, CA). Mass spectrometry-grade porcine pancreatic trypsin, bupropion (BUP), testosterone (TES), and collagenase type I were purchased from Wako Pure Chemicals (Osaka, Japan). TCPOBOP and 6β-hydroxy TES were obtained from Cayman Chemical (Ann Arbor, MI). 4-Hydroxy BUP and DIC-d4 were purchased from Toronto Research Chemicals (Toronto, Canada). 4′-Hydroxy DIC was obtained from Daiichi Pure Chemicals (Tokyo, Japan). Src kinase inhibitor 1 (SKI-1) and U0126 were purchased from Santa Cruz Biotechnology (Dallas, TX). Bond Elut C18 was obtained from Agilent Technologies (Santa Clara, CA). ReverTra Ace was obtained from Toyobo Life Science (Osaka, Japan). Oligonucleotide primers were from Eurofins (Luxembourg, Luxembourg). All other chemicals and solvents were of mass spectrometry-grade or the highest commercially available purity.

Animals and Treatments. Male WT and D mice of C57BL/6 genetic background between 10 and 14 weeks of age were used in this study. PKN1 knock-in mice lacking kinase activity were generated by introducing a T778A point mutation in the catalytic domain, as described previously (Mashud et al., 2017). PKN3 knockout mice were generated as described previously (Mukai et al., 2016). Double-mutant [*PKN1*$^{T778A/T778A}$; *PKN3*$^{-/-}$] mice were generated by mating PKN1 knock-in mice with PKN3 knockout mice. The mice were housed in an air-conditioned room at 22 ± 0.5°C and relative air humidity of 55 ± 10% with a 12-hour lighting schedule (7:00 AM–7:00 PM) and free access to standard laboratory food (MF; Oriental Yeast Co., Ltd., Tokyo, Japan). Mice were treated with BNF (200 mg/kg, i.p., corn oil), PB (100 mg/kg, i.p., saline), TCPOBOP (3 mg/kg, i.p., corn oil), and DEX (75 mg/kg, i.p., corn oil) (Petrick and Klaassen, 2007). Activators for receptor-type transcription factors or vehicles (10 ml/kg), such as corn oil for BNF, TCPOBOP, and DEX and saline for PB, were injected daily at 4:00 PM for 4 days. The different mice were used as control animals for each activator. Animals were anesthetized with isoflurane 24 hours after the last treatment, and the liver was perfused with ice-cold saline and then removed. After flash freezing in liquid nitrogen, each sample was preserved at −80°C until use for RNA extraction and microsome preparation. The protocol was approved by the Committee for the Care and Use of Laboratory Animals of the Faculty of Pharmacy of Kindai University (Osaka, Japan).

Determination of mRNA Levels by Real-Time Reverse-Transcription Polymerase Chain Reaction. Total RNA was extracted from mouse livers using Sepasol-RNA I Super G. mRNA levels were measured by reverse-transcription polymerase chain reaction using SYBR Green as described previously (Kawase et al., 2008, 2013). Polymerase chain reaction was performed under the following conditions: 40 cycles of 95°C for 10 seconds, 55°C for 10 seconds, and 72°C for 30 seconds. The primer sequences for target gene are listed in Table 1. Data were analyzed using the multiplex comparative method with StepOne Software (Thermo Fisher Scientific, Waltham, MA). The internal control β-actin was used to normalize gene expression.

TABLE 1
Primer sequences used in polymerase chain reaction assays.

Gene		Primer Sequence (5′-3′)
Cyp1a1	Forward	AAGTGCAGATGCGGTCTTCT
	Reverse	GAGCACCCAGAGCACTCTTC
Cyp1a2	Forward	ATGGCCAGAGCATGATTTTC
	Reverse	GGGAAAGTTCTTCCCAAAGC
Cyp2b10	Forward	TGGAGATGTGTTCACAGTGC
	Reverse	TTGAAGGTTGGCTCAACGAC
Cyp2c29	Forward	ACAGGAAAACGGATTTGTGC
	Reverse	ATCCCTGATAGGGAGGGATG
Cyp2c37	Forward	AAGAGGAAGACGGCAATCAA
	Reverse	CTGTTGGGGATGAGGTCAAT
Cyp3a11	Forward	ACAAACAAGCAGGGATGGAC
	Reverse	CTCTGGGTCTGTGACAGCAA
Car	Forward	ACAGACCCGGAGTTACCCAA
	Reverse	CAGAAACCGACTTTGGAGCC
Ccrp	Forward	TGAACTGCTGGAGGACGAAGA
	Reverse	AACCGTCCAAGCATCATCAG
Hsp90	Forward	GCTCCTTCGCTATCACACCT
	Reverse	TTGCTCTTTGCTCTCACCAGT
Rxrα	Forward	ACACCAAACATTTCCTGCCG
	Reverse	CGACCCGTTGGAGAGTTGAG
β-Actin	Forward	CATTGCTGACAGGATGCAGAA
	Reverse	CCGATCCACACAGAGTACTTGC

Preparation of Liver Microsomes. Liver microsomes from WT and D mice were prepared as described previously (Uno et al., 2008). Briefly, the homogenized liver was centrifuged at 12,000 × g for 20 minutes, which was followed by 105,000 × g for 60 minutes to obtain a microsomal pellet. Protein concentrations were determined using a BCA protein assay kit (Life Technologies).

Determination of the Metabolic Activity of Cyp1a, Cyp2b, Cyp2c, and Cyp3a in Liver Microsomes. The metabolic activity of liver microsomes was evaluated by the formation of metabolites of typical P450 substrates, as described previously (Uno et al., 2008). PHE *O*-deethylation activity was used to probe for CYP1A. BUP 4-hydroxylation activity was determined as a probe for CYP2B. DIC 4′-hydroxylation activity was determined as a probe for CYP2C. TES 6β-hydroxylation activity was determined as a probe for CYP3A. The initial concentrations of substrates in microsomal incubations containing 100 μg protein of microsomes were: 100 μM of PHE; 20, 100, 200, and 500 μM of BUP; 10 μM of DIC; and 100 μM of TES. The reaction mixtures were incubated for 20 minutes for BUP and TES, 30 minutes for PHE, and 40 minutes for DIC. These incubation times were within the linear range of enzymatic activity determined in preliminary assays. The internal standards were DIC for PHE and BUP, TES, and DIC-d4 for DIC. Sample clean-up was performed by solid-phase extraction using Bond Elut C18 (Agilent Technologies, Santa Clara, CA). Aliquots (30 μl) were injected onto the liquid chromatography–tandem mass spectrometry (LC-MS/MS) system consisting of an LC system (UltiMate 3000 series, Thermo Fisher Scientific) and a TSQ Endura Triple Quadrupole Mass Spectrometer with electrospray ionization (Thermo Fisher Scientific). The analysis was performed using a reverse-phase column (COSMOSIL 5C18-MSII, 4.6 × 150 mm, 5 μm; Nacalai Tesque). The column temperature was set at 40°C, and the autosampler was maintained at 4°C. The mobile phase [8.5 mM ammonium acetate and 0.0075% [v/v] formic acid in water/methanol (50:50, [v/v])] was pumped at a flow rate of 1.0 ml/min. Electrospray ionization was performed in positive ion mode under the following conditions: 3500 V spray voltage, 400°C ion transfer tube temperature, 300°C vaporizer temperature with a nitrogen sheath, and 10 arbitrary units of auxiliary gases. Finnigan Xcalibur software (Thermo Fisher Scientific) was used for data recording and analysis. Quantification was performed using the selected reaction monitoring of the transitions (mass-to-charge ratio, precursor > product) of acetaminophen (152 > 110), 4-hydroxy BUP (256 > 238), 4-hydroxy DIC (312 > 230), 6β-hydroxy TES (305 > 269), DIC (296 > 214), and DIC-d4 (302 > 220). The areas under the metabolite peaks were normalized by the area under each internal standard. V_{max} and Michaelis constant (K_m) for 4-hydroxy BUP formation were obtained by nonlinear least-square regression of the Michaelis-Menten equation using GraphPad Prism 5 (GraphPad Software, La Jolla, CA).

Determination of P450 Expression by LC-MS/MS–Based Targeted Proteomics. LC-MS/MS–based targeted proteomics was performed according to previously described methods (Hersman and Bumpus, 2014; Kawase et al., 2018). Briefly, 50 μg of liver microsomes were digested by trypsin at 37°C for 18 hours, after which samples were desalted with Bond Elut C18. Eluted samples were dried under a vacuum at 50°C and resuspended in 100 μl of the initial mobile phase (4.5% acetonitrile with 0.1% formic acid). A 20-μl aliquot of each sample was injected into the LC-MS/MS system. The surrogate amino acids sequences for targeted proteins, mass-to-charge ratios of precursor ion and product ion, and collision energy were shown in Supplemental Table 1.

Quantitation of Plasma PB Concentrations by LC-MS/MS. The plasma PB concentrations 24 hours after PB treatments (100 mg/kg, i.p., saline) to WT and D mice were determined by LC-MS/MS according to modification method (Kawase et al., 2019). Briefly, a 5-μl plasma was deproteinated by adding 50 μl methanol followed by centrifugation at 2000 × *g* for 10 minutes. DIC (5 μl of a 100-μg/ml stock) was added as an internal standard to supernatant along with 200 μl of distilled H_2O and 500 μl of ethyl acetate. After evaporation to dryness, the residues were each dissolved in 50 μl of LC mobile phase and filtered with a 0.45-μm Millex-LH filter unit (Millipore, Darmstadt, Germany). Aliquots of 20 μl were injected onto the LC-MS/MS. Analysis was performed using a reversed-phase column (COSMOSIL 5C18-ARII, 2.0 × 150 mm, 5 μm; Nacalai Tesque). Column temperature was set at 40°C, and the autosampler was maintained at 4°C. The mobile phase [8.5 mM ammonium acetate and 0.0075% (v/v) formic acid in water/methanol (50:50, v/v)] was pumped at a flow rate of 0.2 ml/min. Electrospray ionization was performed in negative ion mode, under the following conditions: 2500 V spray voltage, 400°C ion transfer tube temperature, 300°C vaporizer temperature with a nitrogen sheath, and 10 arbitrary units of auxiliary gases. Finnigan Xcalibur software was used for data recording and analysis. Quantification was performed using the selected reaction monitoring of the transitions [mass-to-charge ratio, precursor > product, collision energy (V)] of PB (231 > 188, 18 V), and DIC (294 > 250, 15 V). The areas under the PB peaks were normalized by the area under DIC.

Primary Culture of Hepatocytes and Treatments. Mouse hepatocytes were isolated using a two-step collagenase perfusion method as described previously (Seglen, 1976). Viability, as determined by trypan blue exclusion, was above 90%. Hepatocytes were seeded at 1×10^5 cells/cm^2 on a collagen-coated 24-well plate (Sumitomo Bakelite, Tokyo, Japan) in Williams' Medium E supplemented with 10% fetal bovine serum, 100 nM insulin, 100 nM dexamethasone, 100 U/ml penicillin, 100 μg/ml streptomycin, and 2 mM GlutaMAX supplement I. After an initial attachment period of 2 hours, the medium was replaced with fresh serum-free Williams' Medium E with whole supplement and 5 U/ml aprotinin. Hepatocytes were treated with 1 mM PB 1 hour after the addition of SKI-1 (an Src inhibitor) or U0126 [a mitogen-activated protein kinase (MEK) inhibitor] at a concentration of 10 μM. Twenty-four hours after PB treatment, total RNA was extracted from mouse livers using Sepasol-RNA I Super G. mRNA levels of *Cyp2b10* in each group were measured as described above.

Statistical Analysis. Differences in between-group means were analyzed statistically using the Bonferroni test, Dunnett's test after analysis of variance, or unpaired Student's *t* test. GraphPad Prism 5 was used for all statistical analyses. Values of $p < 0.05$ were considered to be statistically significant.

Results

P450 mRNA Levels Were Markedly Increased in D Mice after PB Treatments Compared with WT Mice. To confirm the susceptibility of WT and D mice to the P450

inducers, the mRNA levels of P450s were determined after treatment with activators for receptor-type transcription factors (Fig. 1). We investigated the mRNA levels of P450s in the livers of mice treated with BNF (AhR ligand), PB (indirect activator of CAR), TCPOBOP (direct CAR ligand), and DEX (PXR ligand). In a preliminary study, we confirmed little changes of the P450 induction between untreated versus treated with vehicle control. Although the mean values of P450 mRNA levels were different, the differences in between-group means were not statistically significant. BNF significantly increased the mRNA levels of *Cyp1a1* and *Cyp1a2* in both WT and D mice. The vehicle treatments had little effect on the mRNA levels of P450s (Fig. 1A). After PB treatment, the mRNA levels of *Cyp2b10* and *Cyp3a11* were significantly increased in both WT and D mice compared with the control (Fig. 1B). The mRNA levels of *Cyp2c29* and *Cyp2c37* were significantly increased in D but not WT mice compared with the control (Fig. 1B). There was a significant increase in the mRNA levels of *Cyp2b10*, *Cyp2c29*, and *Cyp2c37* in D mice treated with PB compared with WT mice treated with PB (Fig. 1B). There was a significant increase in the mRNA levels of *Cyp2b10*, *Cyp2c29*, *Cyp2c37*, and *Cyp3a11* in WT mice after treatment with TCPOBOP compared with the control (Fig. 1C). Notably, TCPOBOP, similar to PB, led to a marked increase in the mRNA levels of *Cyp2b10* in both WT and D mice. Importantly, there were differences in the induction of *Cyp2b10* in D mice relative to WT mice after treatment with different CAR activators. PB, an indirect activator of CAR, significantly increased the mRNA levels of *Cyp2b10* in D mice compared with WT mice (Fig. 1B), and TCPOBOP, a direct CAR ligand in mice, increased the mRNA level of *Cyp2b10* to a similar extent between WT and D mice (Fig. 1C). The mRNA levels of *Cyp2b10* and *Cyp3a11* but not *Cyp2c29* and *Cyp2c37* were increased in both WT and D mice after DEX treatment (Fig. 1D). Expression of *Cyp3a11* mRNA was higher in D mice compared with WT mice (Fig. 1D). Taken together, these results demonstrate that P450 mRNA inducibility depending on the type of activators for receptor-type transcription factors was different between WT and D mice.

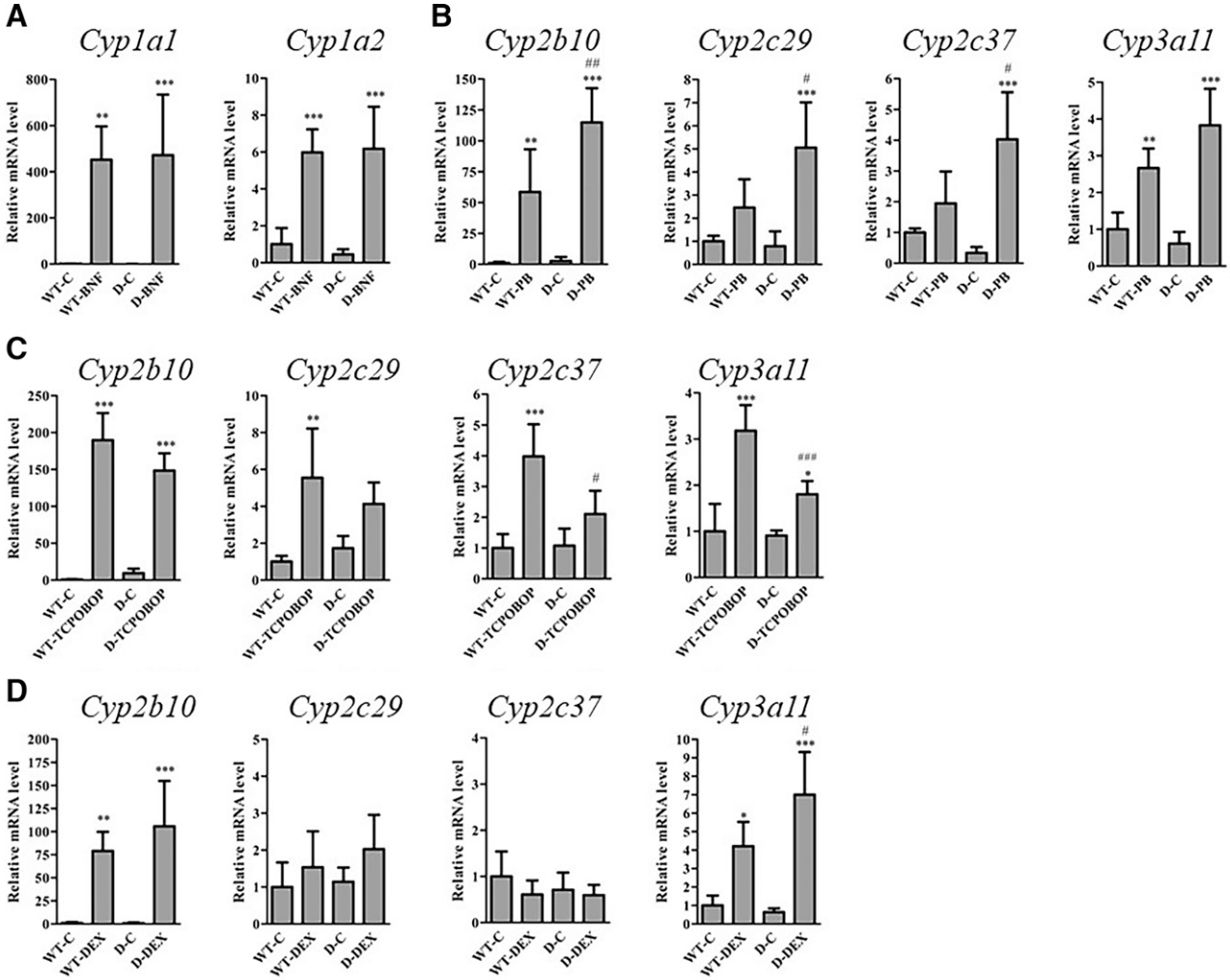

Fig. 1. mRNA levels of *Cyp1a1*, *Cyp1a2*, *Cyp2b10*, *Cyp2c29*, *Cyp2c37*, and *Cyp3a11* in the liver of WT and D mice with or without the treatment with BNF (200 mg/kg, i.p., corn oil) (A), PB (100 mg/kg, i.p., saline) (B), TCPOBOP (3 mg/kg, i.p., corn oil) (C), or DEX (75 mg/kg, i.p., corn oil) (D) for 4 days relative to WT-C. The results are expressed as the mean ± S.D. of each group (BNF, $n = 5$; PB, $n = 5-8$; TCPOBOP, $n = 3-5$; DEX, $n = 4-5$). Differences in between-group means were analyzed statistically using the Bonferroni test after analysis of variance. Significant differences (* $p < 0.05$, ** $p < 0.01$, and *** $p < 0.001$) between control and activator treatments in WT or D mice were observed. Significant differences (# $p < 0.05$, ## $p < 0.01$, and ### $p < 0.001$) between WT mice treated with activator and D mice treated with activator were observed.

P450 Protein Levels Were Higher in D Mice after PB Treatment Compared with WT Mice. Changes in the mRNA levels of P450s did not necessarily correspond to changes in the protein expression of P450s. To determine the effects of BNF, PB, TCPOBOP, and DEX on the protein levels of P450s, liver microsomes from WT and D mice were examined in the absence and presence of treatment with these activators (Fig. 2; Supplemental Tables 2–5). The protein levels of CYP1A1 in liver microsomes from both WT and D mice significantly increased after BNF treatment (Fig. 2A). The protein levels of CYP1A2 in the liver microsomes of D but not WT mice significantly increased after BNF treatment (Fig. 2A). The protein levels of CYP2B10, CYP2C29, and CYP3A11 in the liver microsomes of D mice were significantly increased after PB treatment (Fig. 2B). The protein levels of CYP2B10 in microsomes from D mice were higher than those in microsomes from WT mice after treatment, similar to the changes in observed *Cyp2b10* mRNA levels (Fig. 2B). The protein levels of CYP2B10 and CYP2C29 were increased significantly in the liver microsomes of WT and D mice to a similar extent after treatment of TCPOBOP (Fig. 2C). There were few changes in the protein levels of P450s in the liver microsomes of WT and D mice after DEX treatment (Fig. 2D). Changes in the protein levels of other P450s were smaller compared with those of the marker P450s (Supplemental Tables 2–5). These results suggest that the inducibility of P450s protein as well as mRNA depending on the type of activators for receptor-type transcription factors was different between WT and D mice.

CYP2B Activity Was Higher in D Mice after PB Treatment Compared with WT Mice. Next, the metabolic activity of PHE *O*-deethylation by CYP1A after BNF treatment (Fig. 3A); BUP 4-hydroxylation by CYP2B, DIC 4′-hydroxylation by CYP2C, and TES 6β-hydroxylation by CYP3A after PB treatment (Fig. 3B); BUP 4-hydroxylation by CYP2B after TCPOBOP treatment (Fig. 3C); and TES 6β-hydroxylation by CYP3A after DEX treatment (Fig. 3D) were determined in liver microsomes from WT and D mice. The metabolic activity of PHE *O*-deethylation after BNF treatment; BUP 4-hydroxylation after PB or TCPOBOP treatment; and TES 6β-hydroxylation after PB treatment were significantly increased in WT and D mice compared with the control (Fig. 3). BUP 4-hydroxylation in D mice was significantly

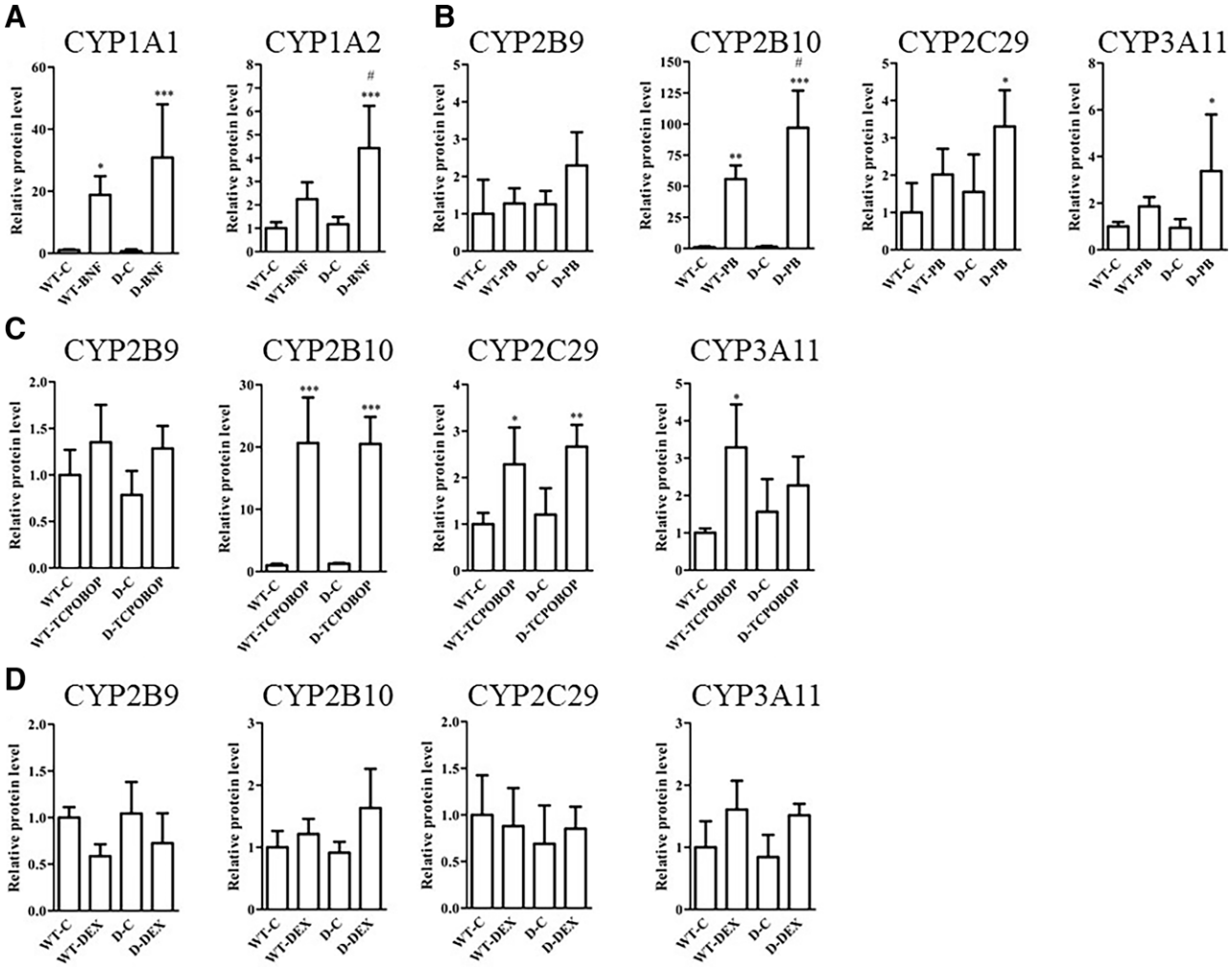

Fig. 2. Protein levels of CYP1A1, CYP1A2, CYP2B9, CYP2B10, CYP2C29, and CYP3A11 in liver microsomes from WT and D mice with or without treatment with BNF (200 mg/kg, i.p., corn oil) (A), PB (100 mg/kg, i.p., saline) (B), TCPOBOP (3 mg/kg, i.p., corn oil) (C), or DEX (75 mg/kg, i.p., corn oil) (D) for 4 days relative to WT-C. The results are expressed as the mean ± S.D. of each group (BNF, $n = 5$; PB, $n = 5$; TCPOBOP, $n = 3-5$; DEX, $n = 4-5$). Differences in between-group means were analyzed statistically using the Bonferroni test after analysis of variance. Significant differences (* $p < 0.05$, ** $p < 0.01$ and *** $p < 0.001$) between control and activator treatments in WT or D mice were observed. Significant differences (# $p < 0.05$) between WT mice treated with activator and D mice treated with activator were observed.

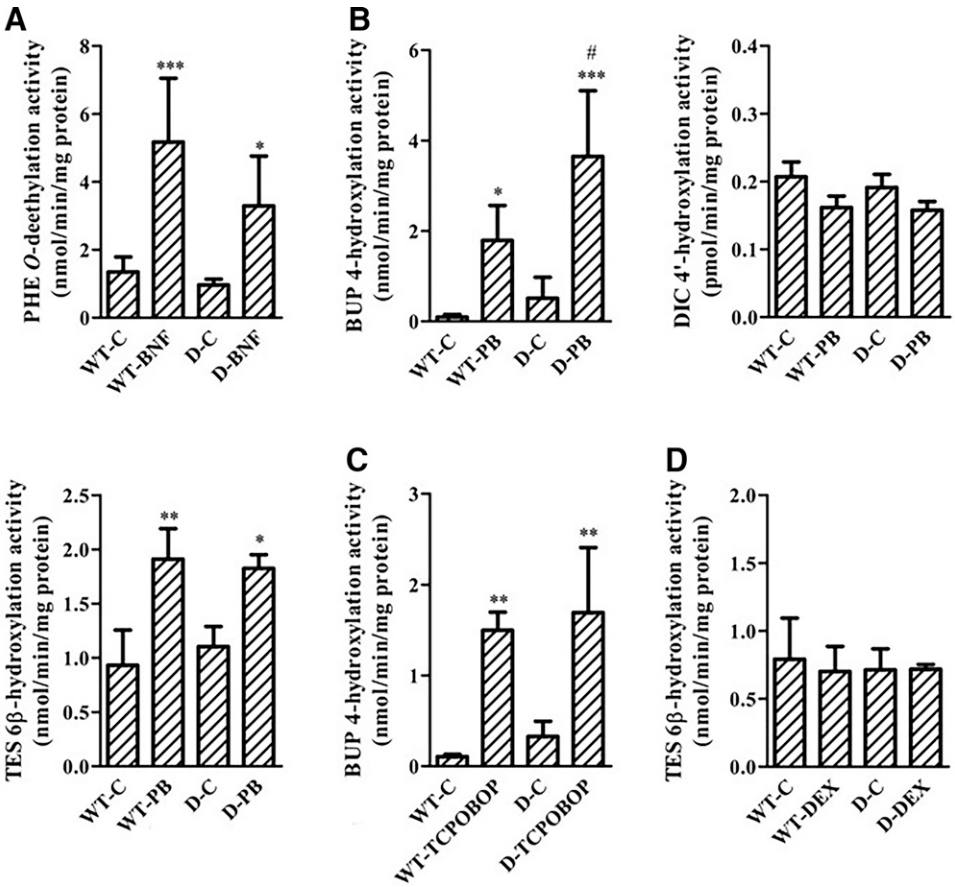

Fig. 3. Metabolic activity of PHE *O*-deethylation after BNF treatment (200 mg/kg, i.p., corn oil) (CYP1A) (A); BUP 4-hydroxylation (CYP2B), DIC 4′-hydroxylation (CYP2C), and TES 6β-hydroxylation (CYP3A) after PB treatments (100 mg/kg, i.p., saline) (B); BUP 4-hydroxylation (CYP2B) after TCPOBOP treatments (3 mg/kg, i.p., corn oil) (C); and TES 6β-hydroxylation (CYP3A) after DEX treatments (75 mg/kg, i.p., corn oil) (D) for 4 days in the liver microsomes of WT and D mice. The results are expressed as the mean ± S.D. of each group (BNF, $n = 5$; PB, $n = 3-5$; TCPOBOP, $n = 3-5$; DEX, $n = 4-5$). Differences in between-group means were analyzed statistically using the Bonferroni test after analysis of variance. Significant differences (* $p < 0.05$, ** $p < 0.01$, and *** $p < 0.001$) between control and activator treatments in WT or D mice were observed. Significant differences (# $p < 0.05$) between WT mice treated with activator and D mice treated with activator were observed.

higher than that in WT mice after treatment with PB (Fig. 3B). However, similar induction of BUP 4-hydroxylation was observed in WT and D mice after treatment with TCPOBOP. DIC 4′-hydroxylation after PB treatment and TES 6β-hydroxylation after DEX treatment were unchanged (Fig. 3, B and D). BUP 4-hydroxylation is slightly catalyzed by CYP2D and CYP3A, although BUP 4-hydroxylation activity is widely used as a marker of CYP2B activity (Dickmann et al., 2012; Maximos et al., 2017; Zhou et al., 2017). Therefore, BUP 4-hydroxylation activity reflects the activities of major CYP2B and minor CYP2D and CYP3A. The inducibility of CYP2B mRNA, protein, and activity in D mice was different between PB and TCPOBOP treatments. To clarify the effects of functional PKN1/PKN3 deficiency on the characteristics of CYP2B in liver microsomes from WT and D mice with or without PB or TCPOBOP, Michaelis-Menten kinetics of 4-hydroxy BUP formation by CYP2B were examined after treatment with PB (Fig. 4A) or TCPOBOP (Fig. 4B). V_{max} values for the formation of 4-hydroxy BUP by CYP2B in WT and D mice after treatment with PB were 2.28 ± 0.68 and 6.13 ± 1.30 nmol/min/mg protein, respectively ($p < 0.05$). V_{max} values in WT and D mice after treatment with TCPOBOP were 2.36 ± 0.53 and 3.64 ± 0.65 nmol/min/mg protein, respectively. There were no significant changes in the K_m values for 4-hydroxy BUP formation by CYP2B in WT and D mice after treatment with PB or TCPOBOP. V_{max} values in D mice after treatment with PB but not TCPOBOP were higher than those in WT mice. Among these control groups, there was no difference between V_{max} and K_m values. These results suggest that differences in CYP2B10 mRNA and protein expression between WT and D mice after PB treatment affect the activity of CYP2B. The plasma concentrations of PB, which affect the toxicity and inducibility of P450s, were determined. The plasma concentrations of PB 24 hours after intraperitoneal administration to WT and D were 13.9 ± 1.06 μg/ml and 12.7 ± 1.23 μg/ml, respectively.

mRNA Levels of Car-Interacting Proteins Were Not Altered in WT and D Mice Regardless of PB or TCPOBOP Treatment. To confirm changes in the mRNA levels of *Car* and CAR-interacting proteins in WT and D mice with or without CAR activator treatment, the mRNA levels of *Car* and CAR-interacting proteins were determined in the livers of WT and D mice after treatment with PB or TCPOBOP (Fig. 5). In the cytoplasm, CAR forms in complex with cytoplasmic CAR retention protein (CCRP) and heat shock protein (HSP) 90. After dissociation of CAR from CCRP and HSP90 by binding of the CAR ligand, CAR is translocated into the nuclear compartment, where it forms a heterodimer with the retinoid

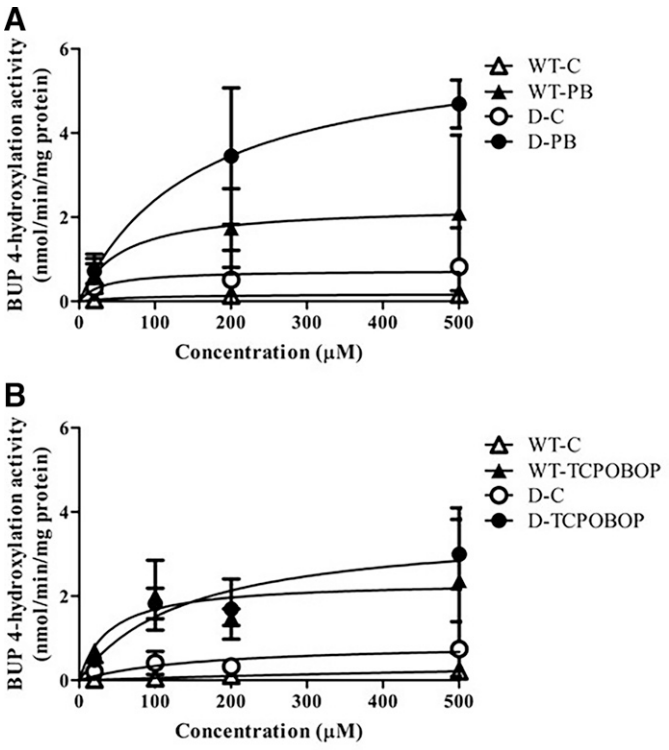

Fig. 4. Michaelis-Menten plots for BUP hydroxylation in liver microsomes from WT and D mice after treatment with PB (100 mg/kg, i.p., saline) (A) or TCPOBOP (3 mg/kg, i.p., corn oil) (B) for 4 days. The results are expressed as the mean ± S.D. of each group (PB, $n = 4-5$; TCPOBOP, $n = 3-5$).

X receptor (RXR) α. The mRNA levels of *Car*, *Ccrp*, *Hsp90*, and *Rxrα* were unchanged in WT and D mice regardless of PB (Fig. 5A) or TCPOBOP treatment (Fig. 5B). Similar mRNA levels of *AhR* and *Pxr* in the livers of WT and D mice with or without PB or TCPOBOP treatments were observed (unpublished data). Taken together, these data indicate that differences in the induction of CYP2B10 between WT and D mice after PB treatment may not be due to the changes in CAR-interacting proteins.

Cyp2b10 mRNA Levels Were Higher in Hepatocytes from D Mice Compared with Those from WT Mice Due to Inhibition of the MEK–Extracellular Signal-Regulated Kinase Pathway. The involvement of PKN in the CAR-dependent pathway after treatment with PB was examined. This was because differences in the CAR-mediated induction of *Cyp2b* in WT and D mice were observed after treatment with PB, an indirect activator of CAR, and TCPOBOP, a direct CAR ligand in mice. Inhibition of EGFR signaling with PB leads to CAR activation and subsequent induction of P450 transcription (Fig. 6A) (Li et al., 2009; Mutoh et al., 2013; Kobayashi et al., 2015; Yan et al., 2015; Negishi, 2017). PB promotes the transformation of receptor for activated C kinase 1 (RACK1) from phosphorylated-RACK (p-RACK) and extracellular signal-regulated kinase (ERK) from phosphorylated-ERK (p-ERK), which is followed by translocation of CAR to the nucleus. To clarify the involvement of PKN in the Src-RACK1 and MEK-ERK pathways in the CAR-mediated induction of *Cyp2b*, the mRNA levels of *Cyp2b10* in hepatocytes from WT and D mice were determined after treatment with PB alone or in combination with SKI-1 (an Src inhibitor) or U0126 [a mitogen-activated protein kinase (MEK) inhibitor] (Fig. 6B). The relative mRNA levels of *Cyp2b10* were increased by PB alone and by the combination of PB with SKI-1 or U0126 compared with the control in both WT and D cells (Fig. 6B). The combination of PB and SKI-1 or U0126 in hepatocytes from D mice significantly elevated the mRNA levels of *Cyp2b10* compared with those from WT mice (Fig. 6B). The mRNA levels of *Cyp2b10* were higher in hepatocytes from D mice treated with the combination of PB and U0126 compared with those treated with PB alone (Fig. 6B). The combination of PB and SKI-1 in hepatocytes from D mice resulted in a similar induction of *Cyp2b10* mRNA to PB alone (Fig. 6B). In preliminary experiments, the treatments of SKI-1 alone or U0126 alone had little impact on the mRNA levels of *Cyp2b10* in hepatocytes from WT and D mice (unpublished data).

Discussion

Our present study revealed the roles of PKN in the AhR-, CAR-, and PXR-mediated transcription processes of P450s. After treatment with activators for receptor-type transcription factors, changes in the expression of marker genes, including *Cyp1a1* (AhR), *Cyp2b10* (CAR), *Cyp3a11* (PXR), and other major P450s, were examined in WT and D mice.

The results demonstrated that PKN1 and PKN3 negatively affected the Src-RACK1 pathway in the induction of *Cyp2b10* mediated by CAR. Several lines of evidence support the above-mentioned findings. First, PB markedly increased the mRNA and protein levels and metabolic activity of CYP2B10 in D mice compared with WT mice. Second, TCPOBOP, unlike PB, exhibited little difference in the induction of mRNA, protein, or metabolic activity between WT and D, although both PB and TCPOBOP activated CAR. Finally, inhibition of the MEK-ERK pathway but not the Src-RACK1 pathway before PB treatment after PB treatment significantly increased the mRNA levels of *Cyp2b10* in hepatocytes from D mice compared with those from WT mice. To our knowledge, this is the first study that demonstrates the roles of PKN1 and PKN3 in the in vivo transcriptional induction of P450s.

After treatment with the AhR ligand BNF, there was little difference in the mRNA levels of *Cyp1a1* and *Cyp1a2* between WT and D mice (Fig. 1A). PHE *O*-deethylation activity was observed in WT and D mice after treatment with BNF (Fig. 3), although the protein levels of CYP1A2 in D mice were significantly increased compared with those in the WT and control D mice (Fig. 2A). These results indicate that PKN had little effect on the induction of *Cyp1a1* and *Cyp1a2* by AhR. After treatment with the PXR ligand DEX, the relative mRNA and protein levels of P450s were unchanged between WT and D mice (Figs. 1D, 2D), showing that PKN had little effect on the induction of P450s by PXR. Previous studies demonstrated that the phosphorylation of PXR by protein kinase A exerted inhibitory effects on P450 transcription (Ding and Staudinger, 2005; Lichti-Kaiser et al., 2009; Staudinger et al., 2011). However, PKN is likely to have little impact on the transcriptional regulation of P450s via phosphorylation of PXR. Although DEX is widely used as a PXR ligand in mouse studies (Cheng et al., 2005; Buckley and Klaassen, 2009), pregnenolone-16α-carbonitrile is a rodent-specific and strong ligand of PXR (Guzelian et al., 2006). The further studies using pregnenolone-16α-carbonitrile could help elucidate the roles of PKN in

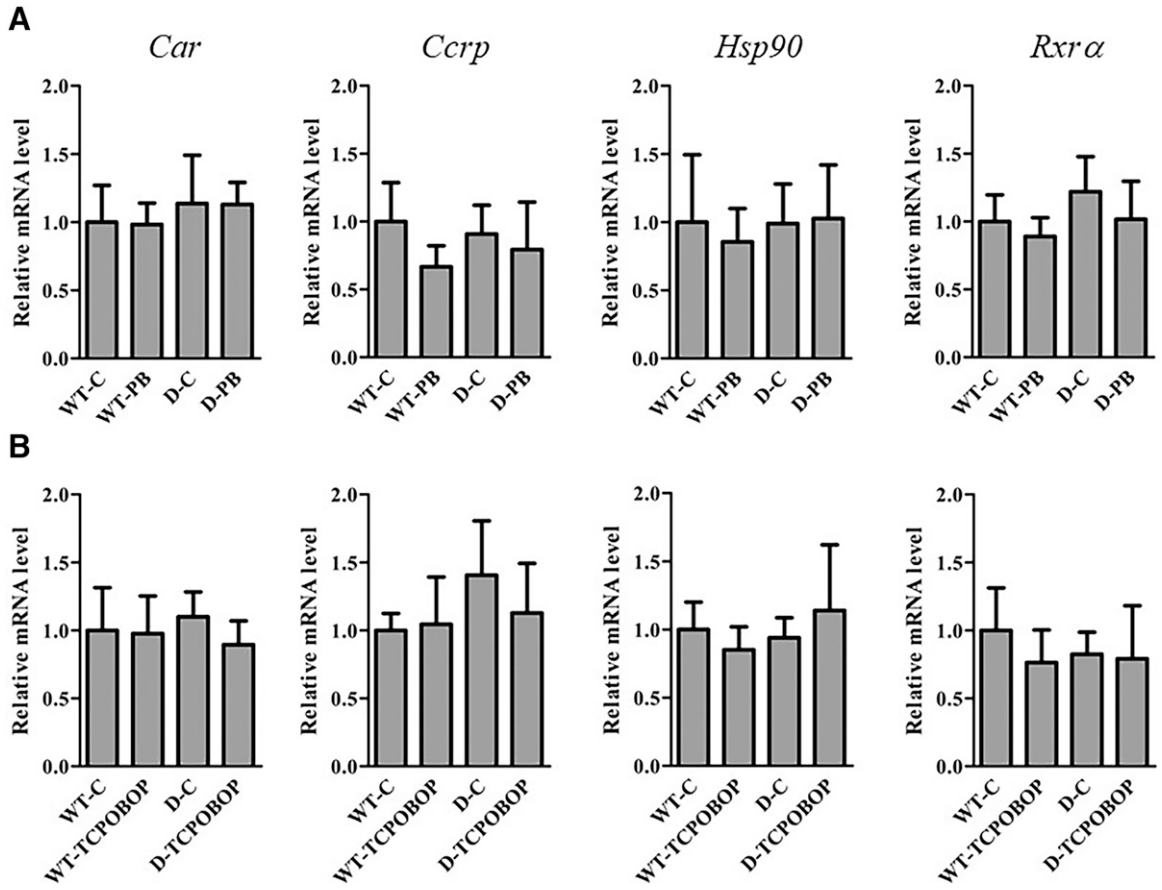

Fig. 5. mRNA levels of Car, Ccrp, Hsp90, and Rxrα in the liver of WT and D mice with or without treatment with PB (100 mg/kg, i.p., saline) (A) or TCPOBOP (3 mg/kg, i.p., corn oil) (B) for 4 days relative to WT-C. The results are expressed as the mean ± S.D. of each group (PB, n = 4; TCPOBOP, n = 3 – 5).

PXR-mediated induction of P450. Also, consideration should be given to the differences of induction kinetics and the half-life of mRNA, protein, and activity of P450s. Further studies are needed to clarify the involvement of PKN in the induction kinetics of mRNA, protein, and activity of P450s. The similar concentrations of PB in WT and D were observed. The predominantly metabolic enzyme for PB is Cyp2c, and the metabolic activities of CYP2C in WT and D treated with PB were unchanged (Fig. 3B). Therefore, the similar extent of PB exposures to WT and D mice could occur.

After treatment with the CAR activator PB and CAR ligand TCPOBOP, there were significant differences in the induction of CYP2B10 mRNA and protein (Figs. 1A, 1B, 2B, and 2C). The treatment of D mice with PB, an indirect activator of CAR, led to a significant induction of CYP2B10 mRNA and protein expression compared with the corresponding WT mice. In the cytoplasm, CAR forms a complex with CCRP and HSP90. After the dissociation of CAR from CCRP and HSP90 by the binding of CAR direct ligands, such as TCPOBOP, CAR translocates to the nuclear compartment. As shown in Fig. 6A, PB inhibits the binding of epidermal growth factor (EGF) to EGFR, which leads to the translocation of CAR to the nucleus and induction of target P450 transcription (Li et al., 2009; Mutoh et al., 2013; Kobayashi et al., 2015). The phosphorylation of CAR-interacting protein is involved in the translocation of CAR to the nucleus (Shizu et al., 2017). Timsit and Negishi (2014) demonstrated that TCPOBOP increased CCRP ubiquitination in human hepatocellular carcinoma HepG2 cells coexpressing CAR. Enhanced proteasomal degradation of CCRP leads to increased translocation of CAR to the nucleus. Thus, TCPOBOP acts directly on CAR complexes in the cytoplasm. Dephosphorylation of Thr-38 in the CAR protein is also important for CAR translocation to the nucleus (Kawamoto et al., 1999; Mutoh et al., 2009; Hori et al., 2016); however, CAR translocation to the nucleus for P450 induction is a common process after treatment with PB and TCPOBOP. Furthermore, there was no change in the mRNA levels of *CAR* and CAR-interacting proteins (Fig. 5), suggesting that differences in the induction of *Cyp2b10* by PB and TCPOBOP were not due to changes in the expression levels of these proteins in WT and D mice. Hence, differences in the induction of *Cyp2b10* between WT and D mice after PB treatment could be illustrated by the phosphorylation of signaling molecules upstream of CAR translocation to the nucleus by PKN.

To determine the involvement of PKN in the CAR-dependent pathway of *Cyp2b10* induction after PB treatment, we examined the mRNA levels of *Cyp2b10* in hepatocytes of WT and D mice treated with PB in combination with inhibitors of signaling pathways . The mRNA levels of *Cyp2b10* in hepatocytes from D mice were higher than those in hepatocytes from WT mice after treatment with PB. Treatment with a combination of PB and U0126 has been shown to increase *Cyp2b10* mRNA levels in primary hepatocytes (Joannard et al., 2006). Inhibition of the MEK-ERK pathway after treatment with PB

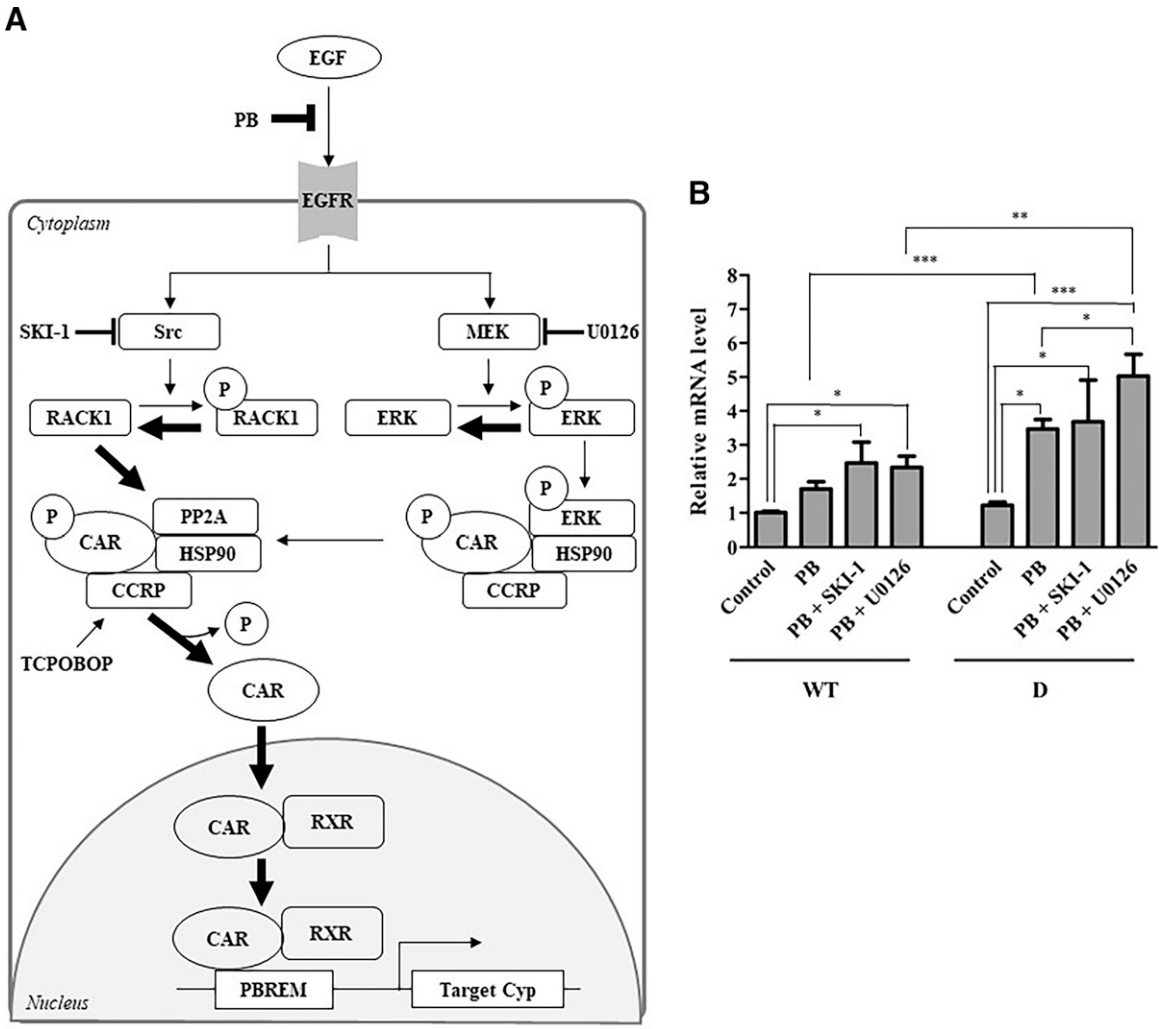

Fig. 6. Inhibition of EGFR signaling by PB leads to CAR activation and subsequent P450 induction (A). PB inhibits EGF-EGFR binding after the transformation of RACK1 from p-RACK and ERK from p-ERK (bold arrows). Subsequently, CAR translocates to the nucleus where it promotes the transcription of target P450s, such as Cyp2b10. PBREM, phenobarbital-responsive enhancer module; PP2A, protein phosphatase 2A. The mRNA levels of *Cyp2b10* in hepatocytes from WT and D mice after PB treatment (1 mM) with or without SKI-1 or U0126 for 24 hours (B) relative to controls of WT. Significant differences (* $p < 0.05$, ** $p < 0.01$, and *** $p < 0.001$) were observed. Significant differences from the control of WT or D mice were analyzed by Dunnett's test after an analysis of variance. Other significant differences of WT or D mice were assessed by an unpaired Student's t test. The results are expressed as the mean ± standard error of each group ($n = 5 - 7$).

and U0126 resulted in marked increases in *Cyp2b10* mRNA levels in hepatocytes from D mice. There were few differences in *Cyp2b10* mRNA levels between hepatocytes from WT and D mice treated with the combination of PB and SKI-1. Based on these results, we believe that PKN could have inhibitory effects on the Src-RACK1 pathway but not the MEK-ERK pathway. Previous reports from our group and other investigators showed increases in Src activity mediated by PKN3 in vitro (Uehara et al., 2017; Gemperle et al., 2019). Higher Src activity promotes the transformation of p-RACK1 from RACK1, which is linked to the suppressed induction of *Cyp2b10* by PB (Fig. 6A). It is also needed to further investigate the effects of the lacking PKN activity on the phosphorylation of RACK1 and ERK after PB treatments. The inhibition of the translocation of CAR to nucleus by inhibitors, such as okadaic acid, provides support for the roles of PKN in CAR-mediated induction of Cyp2b10, although PKN possibly works the signaling processes before CAR translocation to nucleus. A limitation of our study is the detailed mechanisms of the negative regulation of CAR-mediated induction of *Cyp2b10* by PKN1/3, although the results of this study show the possibility of inhibitory effects of PKN on the Src-RACK1 pathway. Further studies are needed to clarify the roles of PKN in the signaling processes of EGF-induced activation of EGFR. A decline in this suppression in D mice could promote the induction of *Cyp2b10* by PB. PB treatments modulate functions of PXR, AMP-activated protein kinase (AMPK), hepatocyte nuclear factor-4α, and the peroxisome proliferator-activated receptor-α (PPAR-α) in addition to CAR in the livers of mice (Shindo et al., 2007; Tamasi et al., 2009; Braeuning and Pavek, 2020). Previous report demonstrated that AMPK participated in PB induction of CYP2B via the modulation of CAR activity (Rencurel et al., 2005). The activation of PPAR-α resulted in CYP2B1/2 induction (Shaban et al., 2005). Therefore, there is possibility that PKN is involved in the phosphorylation of AMPK or PPAR-α–associated proteins because PB is highly nonspecific in CAR-mediated transactivation. Further studies are needed to clarify the roles of PKN in CAR-

mediated induction of *Cyp2b10*. It is unclear whether PKN1 or PKN3 predominantly regulates the CAR-mediated induction of *Cyp2b10* after PB treatment. CAR is also involved in the transcriptional regulation of phase II enzymes, such as UDP-glucuronosyltransferase and transporters, which affect drug metabolism, pharmacokinetics, and toxicokinetics (Haouzi et al., 2000; Maher et al., 2005; Shelby and Klaassen, 2006). Therefore, it is important to elucidate the roles of PKN in transcriptionally CAR-regulating proteins in addition to CYP2B10.

In conclusion, to our knowledge, this is the first report on the involvement of PKN in the transcriptional regulation of P450s. Elucidation of the detailed mechanisms of P450 induction could help to optimize pharmacotherapy and improve drug development because P450 induction affects drug efficacy and leads to adverse reactions. PKN1/3 negatively regulates the CAR-mediated induction of *Cyp2b10*, probably because of the phosphorylation of signaling molecules in the Src-RACK1 pathway.

Authorship Contributions

Participated in research design: Kawase, Mukai, Satoh, Shimada, Sugiura, Iwaki.

Conducted experiments: Kawase, Tateishi, Kuroda, Kazaoka.

Contributed new reagents or analytic tools: Mukai.

Performed data analysis: Kawase, Tateishi, Kuroda.

Wrote or contributed to the writing of the manuscript: Kawase, Mukai, Sugiura, Iwaki.

References

Braeuning A and Pavek P (2020) β-catenin signaling, the constitutive androstane receptor and their mutual interactions. *Arch Toxico* **94**:3983–3991.

Buckley DB and Klaassen CD (2009) Induction of mouse UDP-glucuronosyltransferase mRNA expression in liver and intestine by activators of aryl-hydrocarbon receptor, constitutive androstane receptor, pregnane X receptor, peroxisome proliferator-activated receptor α, and nuclear factor erythroid 2-related factor 2. *Drug Metab Dispos* **37**:847–856.

Che X and Dai W (2019) Aryl hydrocarbon receptor: its regulation and roles in transformation and tumorigenesis. *Curr Drug Targets* **20**:625–634.

Cheng X, Maher J, Dieter MZ, and Klaassen CD (2005) Regulation of mouse organic anion-transporting polypeptides (Oatps) in liver by prototypical microsomal enzyme inducers that activate distinct transcription factor pathways. *Drug Metab Dispos* **33**:1276–1282.

Danno S, Kubouchi K, Mehruba M, Abe M, Natsume R, Sakimura K, Eguchi S, Oka M, Hirashima M, Yasuda H, et al. (2017) PKN2 is essential for mouse embryonic development and proliferation of mouse fibroblasts. *Genes Cells* **22**:220–236.

Dickmann LJ, McBride HJ, Patel SK, Miner K, Wienkers LC, and Slatter JG (2012) Murine collagen antibody induced arthritis (CAIA) and primary mouse hepatocyte culture as models to study cytochrome P450 suppression. *Biochem Pharmacol* **83**:1682–1689.

Ding X and Staudinger JL (2005) Repression of PXR-mediated induction of hepatic CYP3A gene expression by protein kinase C. *Biochem Pharmacol* **69**:867–873.

Down MJ, Arkle S, and Mills JJ (2007) Regulation and induction of CYP3A11, CYP3A13 and CYP3A25 in C57BL/6J mouse liver. *Arch Biochem Biophys* **457**:105–110.

Gampel A, Parker PJ, and Mellor H (1999) Regulation of epidermal growth factor receptor traffic by the small GTPase rhoB. *Curr Biol* **9**:955–958.

Gemperle J, Dibus M, Koudelková L, Rosel D, and Brábek J (2019) The interaction of p130Cas with PKN3 promotes malignant growth. *Mol Oncol* **13**:264–289.

Guzelian J, Barwick JL, Hunter L, Phang TL, Quattrochi LC, and Guzelian PS (2006) Identification of genes controlled by the pregnane X receptor by microarray analysis of mRNAs from pregnenolone 16α-carbonitrile-treated rats. *Toxicol Sci* **94**:379–387.

Haouzi D, Lekéhal M, Moreau A, Moulis C, Feldmann G, Robin MA, Lettéron P, Fau D, and Pessayre D (2000) Cytochrome P450-generated reactive metabolites cause mitochondrial permeability transition, caspase activation, and apoptosis in rat hepatocytes. *Hepatology* **32**:303–311.

Hersman EM and Bumpus NN (2014) A targeted proteomics approach for profiling murine cytochrome P450 expression. *J Pharmacol Exp Ther* **349**:221–228.

Hori T, Moore R, and Negishi M (2016) P38 MAP kinase links CAR activation and inactivation in the nucleus via phosphorylation at threonine 38. *Drug Metab Dispos* **44**:871–876.

Itoh S, Hattori T, Hayashi H, Mizutani Y, Todo M, Takii T, Yang D, Lee JC, Matsufuji S, Murakami Y, et al. (1999) Antiproliferative effect of IL-1 is mediated by p38 mitogen-activated protein kinase in human melanoma cell A375. *J Immunol* **162**:7434–7440.

Joannard F, Rissel M, Gilot D, Anderson A, Orfila-Lefeuvre L, Guillouzo A, Atfi A, and Lagadic-Gossmann D (2006) Role for mitogen-activated protein kinases in phenobarbital-induced expression of cytochrome P450 2B in primary cultures of rat hepatocytes. *Toxicol Lett* **161**:61–72.

Kawamoto T, Sueyoshi T, Zelko I, Moore R, Washburn K, and Negishi M (1999) Phenobarbital-responsive nuclear translocation of the receptor CAR in induction of the CYP2B gene. *Mol Cell Biol* **19**:6318–6322.

Kawase A, Fujii A, Negoro M, Akai R, Ishikubo M, Komura H, and Iwaki M (2008) Differences in cytochrome P450 and nuclear receptor mRNA levels in liver and small intestines between SD and DA rats. *Drug Metab Pharmacokinet* **23**:196–206.

Kawase A, Kaneto A, Ishibashi M, Kobayashi A, Shimada H, and Iwaki M (2019) Involvement of diclofenac acyl-β- d -glucuronide in diclofenac-induced cytotoxicity in glutathione-depleted isolated murine hepatocytes co-cultured with peritoneal macrophages. *Toxicol Mech Methods* **29**:1–8.

Kawase A, Tateishi S, and Kazaoka A (2018) Profiling of hepatic metabolizing enzymes and nuclear receptors in rats with adjuvant arthritis by targeted proteomics. *Biopharm Drug Dispos* **39**:308–314.

Kawase A, Yamada A, Gamou Y, Tahara C, Takeshita F, Murata K, Matsuda H, Samukawa K, and Iwaki M (2013) Increased effects of ginsenosides on the expression of cholesterol 7α-hydroxylase but not the bile salt export pump are involved in cholesterol metabolism. *J Nat Med* **67**:545–553.

Kobayashi K, Hashimoto M, Honkakoski P, and Negishi M (2015) *Regulation of gene expression by CAR: an update. Arch Toxicol* **89**:1045–1055.

Lemaire G, Delescluse C, Pralavorio M, Ledirac N, Lesca P, and Rahmani R (2004) The role of protein tyrosine kinases in CYP1A1 induction by omeprazole and thiabendazole in rat hepatocytes. *Life Sci* **74**:2265–2278.

Li H, Chen T, Cottrell J, and Wang H (2009) Nuclear translocation of adenoviral-enhanced yellow fluorescent protein-tagged-human constitutive androstane receptor (hCAR): a novel tool for screening hCAR activators in human primary hepatocytes. *Drug Metab Dispos* **37**:1098–1106.

Lichti-Kaiser K, Xu C, and Staudinger JL (2009) Cyclic AMP-dependent protein kinase signaling modulates pregnane x receptor activity in a species-specific manner. *J Biol Chem* **284**:6639–6649.

Lin W, Wu J, Dong H, Bouck D, Zeng F-Y, and Chen T (2008) Cyclin-dependent kinase 2 negatively regulates human pregnane X receptor-mediated CYP3A4 gene expression in HepG2 liver carcinoma cells. *J Biol Chem* **283**:30650–30657.

Long WP, Pray-Grant M, Tsai JC, and Perdew GH (1998) Protein kinase C activity is required for aryl hydrocarbon receptor pathway-mediated signal transduction. *Mol Pharmacol* **53**:691–700.

Maesaki R, Shimizu T, Ihara K, Kuroda S, Kaibuchi K, and Hakoshima T (1999) Biochemical and crystallographic characterization of a Rho effector domain of the protein serine/threonine kinase N in a complex with RhoA. *J Struct Biol* **126**:166–170.

Maher JM, Cheng X, Slitt AL, Dieter MZ, and Klaassen CD (2005) Induction of the multidrug resistance-associated protein family of transporters by chemical activators of receptor-mediated pathways in mouse liver. *Drug Metab Dispos* **33**:956–962.

Mashud R, Nomachi A, Hayakawa A, Kubouchi K, Danno S, Hirata T, Matsuo K, Nakayama T, Satoh R, Sugiura R, et al. (2017) Impaired lymphocyte trafficking in mice deficient in the kinase activity of PKN1. *Sci Rep* **7**:7663.

Maximos S, Chamoun M, Gravel S, Turgeon J, and Michaud V (2017) Tissue specific modulation of cyp2c and cyp3a mRNA levels and activities by diet-induced obesity in mice: The impact of type 2 diabetes on drug metabolizing enzymes in liver and extra-hepatic tissues. *Pharmaceutics* **9**:9.

McGraw J and Waller D (2012) Cytochrome P450 variations in different ethnic populations. *Expert Opin Drug Metab Toxicol* **8**:371–382.

Mukai H (2003) The structure and function of PKN, a protein kinase having a catalytic domain homologous to that of PKC. *J Biochem* **133**:17–27.

Mukai H, Muramatsu A, Mashud R, Kubouchi K, Tsujimoto S, Hongu T, Kanaho Y, Tsubaki M, Nishida S, Shioi G, et al. (2016) PKN3 is the major regulator of angiogenesis and tumor metastasis in mice. *Sci Rep* **6**:18979.

Müller F, Weitz D, Derdau V, Sandvoss M, Mertsch K, König J, and Fromm MF (2017) Contribution of MATE1 to renal secretion of the NMDA receptor antagonist memantine. *Mol Pharm* **14**:2991–2998.

Mutoh S, Osabe M, Inoue K, Moore R, Pedersen L, Perera L, Rebolloso Y, Sueyoshi T, and Negishi M (2009) Dephosphorylation of threonine 38 is required for nuclear translocation and activation of human xenobiotic receptor CAR (NR1I3). *J Biol Chem* **284**:34785–34792.

Mutoh S, Sobhany M, Moore R, Perera L, Pedersen L, Sueyoshi T, and Negishi M (2013) Phenobarbital indirectly activates the constitutive active androstane receptor (CAR) by inhibition of epidermal growth factor receptor signaling. *Sci Signal* **6**:ra31.

Negishi M (2017) *Phenobarbital meets phosphorylation of nuclear receptors. Drug Metab Dispos* **45**:532–539.

Numazawa S, Shindo S, Maruyama K, Chibana F, Kawahara Y, Ashino T, Tanaka S, and Yoshida T (2005) Impaired nuclear translocation of CAR in hepatic preneoplastic lesions: association with an attenuated CYP2B induction by phenobarbital. *FEBS Lett* **579**:3560–3564.

Oesch-Bartlomowicz B and Oesch F (2008) Phosphorylation of xenobiotic-metabolizing cytochromes P450. *Anal Bioanal Chem* **392**:1085–1092.

Petrick JS and Klaassen CD (2007) Importance of hepatic induction of constitutive androstane receptor and other transcription factors that regulate xenobiotic metabolism and transport. *Drug Metab Dispos* **35**:1806–1815.

Quétier I, Marshall JJT, Spencer-Dene B, Lachmann S, Casamassima A, Franco C, Escuin S, Worrall JT, Baskaran P, Rajeeve V, et al. (2016) Knockout of the PKN family of Rho effector kinases reveals a non-redundant role for PKN2 in developmental mesoderm expansion. *Cell Rep* **14**:440–448.

Raffetto JD, Vasquez R, Goodwin DG, and Menzoian JO (2006) Mitogen-activated protein kinase pathway regulates cell proliferation in venous ulcer fibroblasts. *Vasc Endovascular Surg* **40**:59–66.

Rencurel F, Stenhouse A, Hawley SA, Friedberg T, Hardie DG, Sutherland C, and Wolf CR (2005) AMP-activated protein kinase mediates phenobarbital induction of CYP2B gene expression in hepatocytes and a newly derived human hepatoma cell line. *J Biol Chem* **280**:4367–4373.

Santel A, Aleku M, Röder N, Möpert K, Durieux B, Janke O, Keil O, Endruschat J, Dames S, Lange C, et al. (2010) Atu027 prevents pulmonary metastasis in experimental and spontaneous mouse metastasis models. *Clin Cancer Res* **16**:5469–5480.
Scheer N, Ross J, Kapelyukh Y, Rode A, and Wolf CR (2010) In vivo responses of the human and murine pregnane X receptor to dexamethasone in mice. *Drug Metab Dispos* **38**:1046–1053.
Schrenk D (1998) Impact of dioxin-type induction of drug-metabolizing enzymes on the metabolism of endo- and xenobiotics. *Biochem Pharmacol* **55**:1155–1162.
Seglen PO (1976) Preparation of isolated rat liver cells. *Methods Cell Biol* **13**:29–83.
Shaban Z, Soliman M, El-Shazly S, El-Bohi K, Abdelazeez A, Kehelo K, Kim HS, Muzandu K, Ishizuka M, Kazusaka A, et al. (2005) AhR and PPARalpha: antagonistic effects on CYP2B and CYP3A, and additive inhibitory effects on CYP2C11. *Xenobiotica* **35**:51–68.
Shelby MK and Klaassen CD (2006) Induction of rat UDP-glucuronosyltransferases in liver and duodenum by microsomal enzyme inducers that activate various transcriptional pathways. *Drug Metab Dispos* **34**:1772–1778.
Sheweita SA (2000) Drug-metabolizing enzymes: mechanisms and functions. *Curr Drug Metab* **1**:107–132.
Shindo S, Numazawa S, and Yoshida T (2007) A physiological role of AMP-activated protein kinase in phenobarbital-mediated constitutive androstane receptor activation and CYP2B induction. *Biochem J* **401**:735–741.
Shizu R, Osabe M, Perera L, Moore R, Sueyoshi T, and Negishi M (2017) Phosphorylated nuclear receptor CAR forms a homodimer to repress its constitutive activity for ligand activation. *Mol Cell Biol* **37**:37.
Smutny T, Hyrsova L, Braeuning A, Ingelman-Sundberg M, and Pavek P (2021) Transcriptional and post-transcriptional regulation of the pregnane X receptor: a rationale for interindividual variability in drug metabolism. *Arch Toxicol* **95**:11–25.
Staudinger JL, Xu C, Biswas A, and Mani S (2011) Post-translational modification of pregnane x receptor. *Pharmacol Res* **64**:4–10.
Steelman LS, Chappell WH, Abrams SL, Kempf RC, Long J, Laidler P, Mijatovic S, Maksimovic-Ivanic D, Stivala F, Mazzarino MC, et al. (2011) Roles of the Raf/MEK/ERK and PI3K/PTEN/Akt/mTOR pathways in controlling growth and sensitivity to therapy-implications for cancer and aging. *Aging (Albany NY)* **3**:192–222.
Tamasi V, Juvan P, Beer M, Rozman D, and Meyer UA (2009) Transcriptional activation of PPARα by phenobarbital in the absence of CAR and PXR, in *Molecular Pharmaceutics*, pp 1573–1581, Mol Pharm.
Timsit YE and Negishi M (2014) Coordinated regulation of nuclear receptor CAR by CCRP/DNAJC7, HSP70 and the ubiquitin-proteasome system. *PLoS One* **9**:e96092.
Tzameli I, Pissios P, Schuetz EG, and Moore DD (2000) The xenobiotic compound 1,4-bis[2-(3,5-dichloropyridyloxy)]benzene is an agonist ligand for the nuclear receptor CAR. *Mol Cell Biol* **20**:2951–2958.
Uehara S, Udagawa N, Mukai H, Ishihara A, Maeda K, Yamashita T, Murakami K, Nishita M, Nakamura T, Kato S, et al. (2017) Protein kinase N3 promotes bone resorption by osteoclasts in response to Wnt5a-Ror2 signaling. *Sci Signal* **10**:eaan0023.
Uno S, Fujii A, Komura H, Kawase A, and Iwaki M (2008) Prediction of metabolic clearance of diclofenac in adjuvant-induced arthritis rats using a substrate depletion assay. *Xenobiotica* **38**:482–495.
Wang Y, Liao M, Hoe N, Acharya P, Deng C, Krutchinsky AN, and Correia MA (2009) A role for protein phosphorylation in cytochrome P450 3A4 ubiquitin-dependent proteasomal degradation. *J Biol Chem* **284**:5671–5684.
Yan J, Chen B, Lu J, and Xie W (2015) *Deciphering the roles of the constitutive androstane receptor in energy metabolism. Acta Pharmacol Sin* **36**:62–70.
Yoshinari K, Kobayashi K, Moore R, Kawamoto T, and Negishi M (2003) Identification of the nuclear receptor CAR:HSP90 complex in mouse liver and recruitment of protein phosphatase 2A in response to phenobarbital. *FEBS Lett* **548**:17–20.
Zhou L, Zhang W, Xie W, Chen H, Yu W, Li H, and Shen G (2017) Tributyl phosphate impairs the urea cycle and alters liver pathology and metabolism in mice after short-term exposure based on a metabonomics study. *Sci Total Environ* **603-604**:77–85.

Address correspondence to: Masahiro Iwaki, Ph.D., Department of Pharmacy, Faculty of Pharmacy, Kindai University, 3-4-1 Kowakae, Higashi-osaka, 577-8502 Osaka, Japan. E-mail: iwaki@phar.kindai.ac.jp; or Hideyuki Mukai, Ph.D., Department of Clinical Laboratory, Kitano Hospital, 530-8480 Osaka, Japan, and Biosignal Research Center, Kobe University, 657-8501 Hyogo, Japan. E-mail: mukinase@kobe-u.ac.jp